

pacs64.60.Ak, 05.10.Ln, 05.70.Jk

# The Tails of the crossing probability

Oleg A.Vasilyev\*

*L.D.Landau Institute for Theoretical Physics RAS,  
142432, Chernogolovka, Moscow reg., Russia*

(Dated: December 2, 2024)

The scaling of the tails of the probability of a system to percolate only in the horizontal direction  $\pi_{hs}$  was investigated numerically for correlated site-bond percolation model for  $q = 1, 2, 3, 4$ . We have proved that the tails of the crossing probability far from the critical point have shape  $\pi_{hs}(p) \simeq \exp(cL [p - p_c]^\nu)$  where  $\nu$  is the correlation length index,  $p = 1 - \exp(-\beta)$  is the probability of a bond to be closed. Near the criticality we observe crossover to another scaling  $\pi_{hs}(p) \simeq A \exp(-b \{L[p - p_c]^\nu\}^z)$ . Here  $z$  is a scaling index describing the central part of the crossing probability.

## I. INTRODUCTION

The  $q$ -state Potts model can be represented as the correlated site-bond percolation in terms of Fortuin-Kasteleyn clusters [1]. At the critical point of the second order phase transition, the infinite cluster is formed. This cluster cross the system connecting the opposite sides of the square lattice. In the last decade the study of the shape of the crossing probability was performed as by conformal methods [2, 3, 4, 5, 6, 7] as well as numerically [8, 9, 10, 11, 12, 13, 14, 15, 16, 17].

According Refs. [20, 21] the distribution function of the percolation thresholds is Gaussian function. Following the number of works [10, 16, 17, 18, 19] the tails of the distribution function are not Gaussian one. The authors of the recent work Ref. [22] are still uncertain to distinguish a stretched exponential behavior from a Gaussian.

The aim of this paper is to investigate the shape of the probability of a system to percolate only in horizontal direction  $\pi_{hs}$ . We perform numerical simulation of correlated site-bond

---

\*Electronic address: vasilyev@itp.ac.ru

percolation model for  $q = 1, 2, 3, 4$  (the percolation model  $q = 1$ , the Ising model  $q = 2$ , and the Potts model  $q = 3, 4$ ) for lattice sizes  $L = 32, 48, 64, 80, 128$ . The scaling formula for a body of the crossing probability near criticality and for tails of the crossing probability was obtained. The final result for the representative case  $q = 2$ ,  $L = 128$  is immediately presented in Fig.1a). Details of fitting procedure are described in Section IV. In this figure

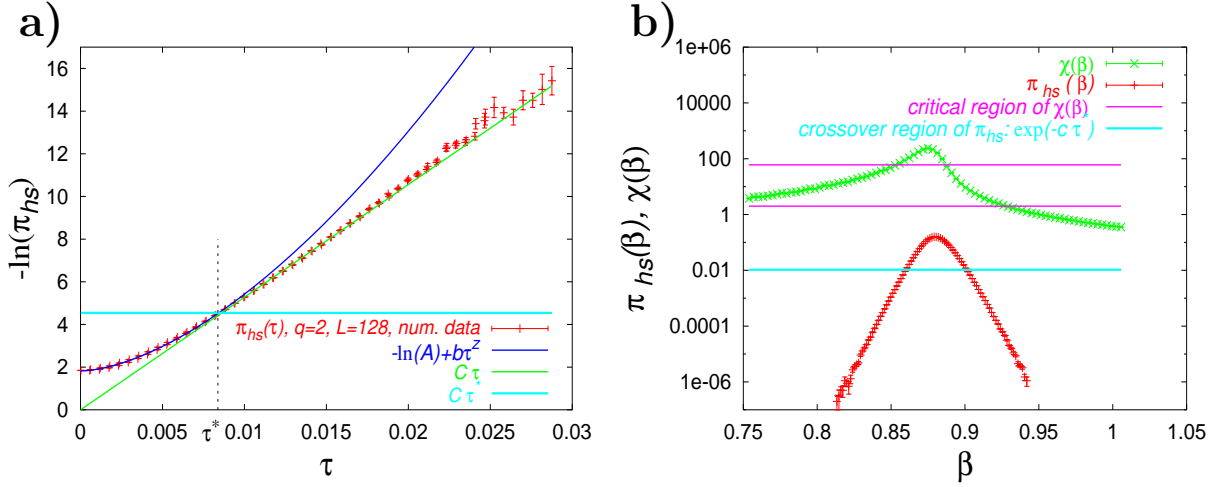


FIG. 1: a) The absolute value of the logarithm of the crossing probability  $-\ln(\pi_{h_s})$  for the Ising model as a function of the absolute value of the scaling variable  $\tau = L(p - p_c)^\nu$ ; b) The magnetic susceptibility  $\chi(\beta)$  and the crossing probability  $\pi_h(\beta)$  as a functions of  $\beta$  inverse temperature  $\beta$  for the Ising model;

we plot (by red crosses) the numerical data for the absolute value of the logarithm of crossing probability  $\pi_{h_s}$  for the Ising model ( $q = 2$ ) on the lattice  $L = 128$  as a function of the absolute value of the scaling variable  $\tau = L(p - p_c)^\nu$ . Here  $p = 1 - \exp(-\beta)$  is a probability of bond to be closed,  $\beta$  is the inverse temperature,  $\nu$  is the correlation length scaling index. The critical point in the  $p$  scale for the  $q$ -state Potts model is  $p_c = \sqrt{q}/(1 + \sqrt{q})$  see Ref. [23] and we get  $p_c(q = 2) \simeq 0.58578\dots$

We can see from Fig.1 that the function  $\pi_{h_s}(\tau)$  consists of two parts: the body  $|\tau| < \tau^*$  and the tails  $|\tau| > \tau^*$ . The body of the crossing probability as a function of  $\tau$  is well described by function  $\ln(A) + b|\tau|^z$  (blue line on the Fig.1a)). Here  $z$  is some scaling index and the value of the crossing probability at the critical point  $\pi_{h_s}(p_c) = A$  may be computed (at least for percolation) by conformal field methods [4]. The logarithms of the tails of the crossing probability have shape  $-C\tau$  (green line in the Fig.1a)). This line is tangent to the body at the point  $\tau^*$ . This point is marked by the horizontal cyan line. Let us note that in Fig.1a)

we plot two branches of the crossing probability (for  $\tau > 0$  and  $\tau < 0$ ). The coincidence of this two branches indicate the remarkable symmetry of the crossing probability with respect to the variable  $\tau$ .

In Fig.1b) we plot the crossing probability (bottom) and the magnetic susceptibility (top) as a functions of the inverse temperature  $\beta$  with logarithm scale for the ordinate axis. In Fig.1b) we denote the crossover points of  $\pi_{hs}$  by horizontal cyan line too. For the magnetic susceptibility we mark the region with critical behavior

$$\chi(\beta) \sim ((\beta - \beta_c)/\beta_c)^{-\gamma} \quad (1)$$

by the horizontal magenta lines. We see from Fig.1 that tails of the crossing probability directly corresponds the critical region of magnetic susceptibility. In this critical region the correlation length  $\xi$  is smaller than the sample size  $\xi < L$ . As the temperature approaches to the critical point, the correlation length reaches the sample size. At that point the magnetic susceptibility on the finite lattice deviates from the critical behavior eq. (1) and becomes smoothed – see the region over the top magenta line in the Fig.1b). At the same point the crossing probability crossovers from tails to body – the region over the cyan line in Fig.1b) (and the region *under* the cyan line in Fig.1a)). At the critical point  $\beta_c = -\ln(1 - p_c) \simeq 0.881373\dots$  both the magnetic susceptibility and the crossing probability reach the maximum.

The detailed description of the fitting procedure as well as numerical data for  $q = 1, 2, 3, 4$  are presented below. The main numerical result of this paper is the proving of the formula  $\exp(b[p - p_c]L^\nu)$  for the tails of the crossing probability. Therefore, we pay special attention to fitting procedures.

The paper is organized as follows. In the second section we describe details of the numerical simulation. In the third section the method for determination of the pseudocritical point  $p_c(L, q)$  on the finite lattice is described. We use  $p_c(L, q)$  to perform the approximation of the tails. In section IV we approximate the crossing probability  $\pi_{hs}(p; L, q)$  tails by the function  $\exp(-C(L, q)(p - p_c(L, q))^{x(L, q)})$ . We get  $x(L, q) \simeq \nu(q)$  for this approximation procedure. In section V we describe new fitting procedure based on the using the scaling variable  $\tau = L(p - p_c)^\nu$ . Results of approximation are discussed in Section VI.

## II. DETAILS OF NUMERICAL SIMULATION

We perform the massive Monte-Carlo simulation on the square lattice of size  $L$  to obtain the the high-precision data for  $\pi_{hs}$ . We use the dual lattice shown in Fig. 2. On such lattice the critical point of the bond percolation ( $q = 1$ ) is exactly equal  $1/2$  and is not depend on the lattice size [24]. To produce the pseudorandom numbers we use the R9689 random number generator with four taps [25]. We close each bond with a probability  $p$  and leave it open with a probability  $1 - p$ . Then we split the lattice into clusters of connected sites by using the Hoshen-Kopelman algorithm [26]. After that we check the percolation through this configuration. We average the crossing probability over  $10^7$  random bond configurations. To investigate the Potts model  $q = 2, 3, 4$  we use the Wolff [27] cluster

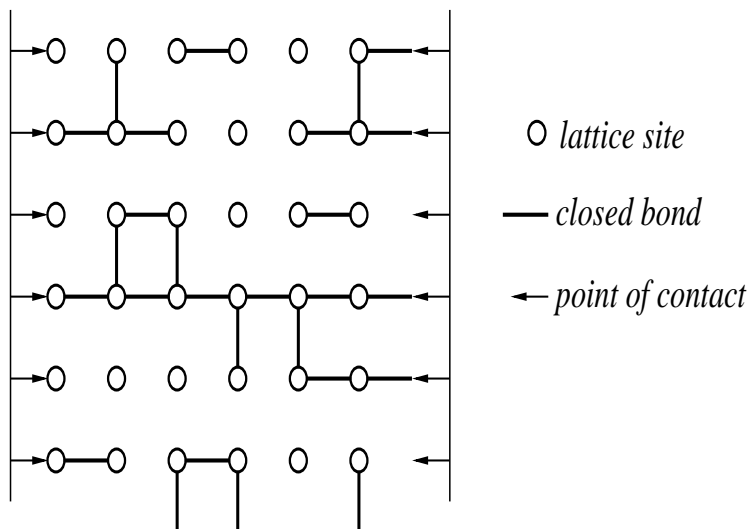


FIG. 2: The dual lattice with the horizontally spanning cluster

algorithm to generate a sequence of thermally equilibrated spin configurations. For each particular inverse temperature  $\beta = \frac{1}{T}$  we flip 20000 Wolff clusters to equilibrate the system. For the spin model on the finite lattice the deviation of the pseudocritical point from the position of the critical point on the infinite lattice is smaller for Periodic Boundary Condition (PBC) rather for Open Boundary Condition [28, 29]. For this reason we use the PBC. For a generated spin configuration we create a configuration of bonds. Each bond between sites with equal spin variable  $\sigma$  is closed with the probability  $p = 1 - \exp(-\beta)$  and is open with probability  $1 - p = \exp(-\beta)$ . Bonds between sites with different values of  $\sigma$  are always

open in accordance with Fortuin-Kasteleyn rule [1]. Then we split the particular spin and bond configurations into different clusters. Then we check the percolation through a new cluster configuration and so on. We average the crossing probability over  $10^7$  configurations for each value of the inverse temperature  $\beta$ . So the resolution of our computations is about  $10^{-7}$ . By this way we perform numerical simulation and get a set of data for  $\pi_{hs}(p; L, q)$  for the lattice sizes  $L = 32, 48, 64, 80, 128$  and  $q = 2, 3, 4$ . The formal definition of  $\pi_{hs}(p; L, q)$  as a sum over different cluster configurations is described in [30].

For the Potts model we use the dual lattice as we do for the percolation. It means, that we take into account additional bonds attached to the bottom row of spins. This bonds connect the bottom and the top rows of spins on the lattice with PBC. In the same way we take into account additional bonds attached to the right column of the spins. This bonds connect the right and the left columns on the lattice with PBC. In Fig.2 contact points are shown by arrows. The left contact points attached to left column of sites. The right contact points attached to the additional bonds. In Fig.2 the bond configuration with the horizontally spanning cluster is shown. Then check the percolation through the obtained cluster configuration. After that we flip three Wolff clusters.

### III. DETERMINATION OF THE PSEUDOCRITICAL POINT ON FINITE LATTICES

We investigate the crossing probability as a function of deviation from the critical point. Therefore, we perform the preliminary approximations to obtain the critical points for the finite samples. Namely, we

- obtain the pseudocritical point and the shape of the central part of the crossing probability
- determine the shape of the tails of the crossing probability
- combine together the information for body and tails and reconstruct the total shape of the crossing probability

Recall that we consider the crossing probability as a function of the variable  $p = 1 - \exp(-\beta)$  (probability of a bond to be closed). It is easily to understand that we must take

the pseudocritical point on the finite lattice  $p_c(L, q)$  as the reference point. The crossing probability is a symmetric function of the variable  $\Delta p = (p - p_c(L, q))$ . This fact implies that the high temperature tail  $p_c - \Delta p$  ( $\Delta p > 0$ ) and the low temperature tail  $p_c + \Delta p$  are coincide  $\pi_{hs}(p_c - \Delta p) = \pi_{hs}(p_c + \Delta p)$ . For the bond percolation on the dual lattice the position of the percolation point does not depend on the lattice size  $p_c(L, q = 1) = 0.5$  [24].

For the determination of  $p_c(L, q)$  for the Ising and the Potts model we use the following procedure. We can assume [30] that in the region  $-6 < \ln(\pi_{hs}(p; L, q))$  the fitting formula is true

$$F(p; L, q) = A(q, L) \exp(-[B(L, q)(p - p_c(L, q))]^{\zeta(L, q)}) \quad (2)$$

Therefore we fit the logarithm of the crossing probability  $\ln(\pi_{hs})$  by the function

$$f_1(p; L, q) = \ln(F(p; L, q)) = a(L, q) - [B(L, q)(p - p_c(L, q))]^{\zeta(L, q)} \quad (3)$$

where  $a(L, q) = \ln(A(L, q))$ . We plot the data for  $\ln(\pi_{hs}(p; L, q))$  as a function of  $p$  in Fig.3a), Fig.3b), Fig.3c), Fig.3d) for  $q = 1, 2, 3, 4$  respectively. The errorbars in this figures are about the symbol size. Results of the approximation are plotted in the same figures by lines. We shall see that there is a good agreement between the numerical data and the results of the approximation. Finally for each pair  $(L, q)$  we obtain the four fitting parameter  $A(L, q)$ ,  $B(L, q)$ ,  $p_c(L, q)$ ,  $\zeta(L, q)$ . Here  $A(L, q)$  define the crossing probability in the critical point,  $B(L, q)$  is a scaling variable,  $p_c(L, q)$  is the position of the pseudocritical point  $p_c(L, q)$  on the lattice  $L$ , and  $\zeta(L, q)$  is a scaling index.

In Table I we collect data for the logarithm of critical amplitude  $a(L, q) = \ln(A(L, q))$ . The fitting parameter  $a(L, q)$  define the shift of graphs in Fig.3a)-3d) from the zero level. This data will be used in the further approximations. We approximate the data for  $B(L, q)$

TABLE I: Results of the approximation for the fitting parameter  $a(L, q) = \ln(A(L, q))$

$L$	$q = 1$	$q = 2$	$q = 3$	$q = 4$
32	-1.689(7)	-1.725(19)	-1.796(31)	-1.921(37)
48	-1.688(8)	-1.726(19)	-1.803(32)	-1.937(40)
64	-1.691(6)	-1.727(20)	-1.812(33)	-1.953(40)
80	-1.692(11)	-1.728(21)	-1.809(36)	-1.961(42)
128	-1.684(15)	-1.728(22)	-1.813(37)	-1.979(41)

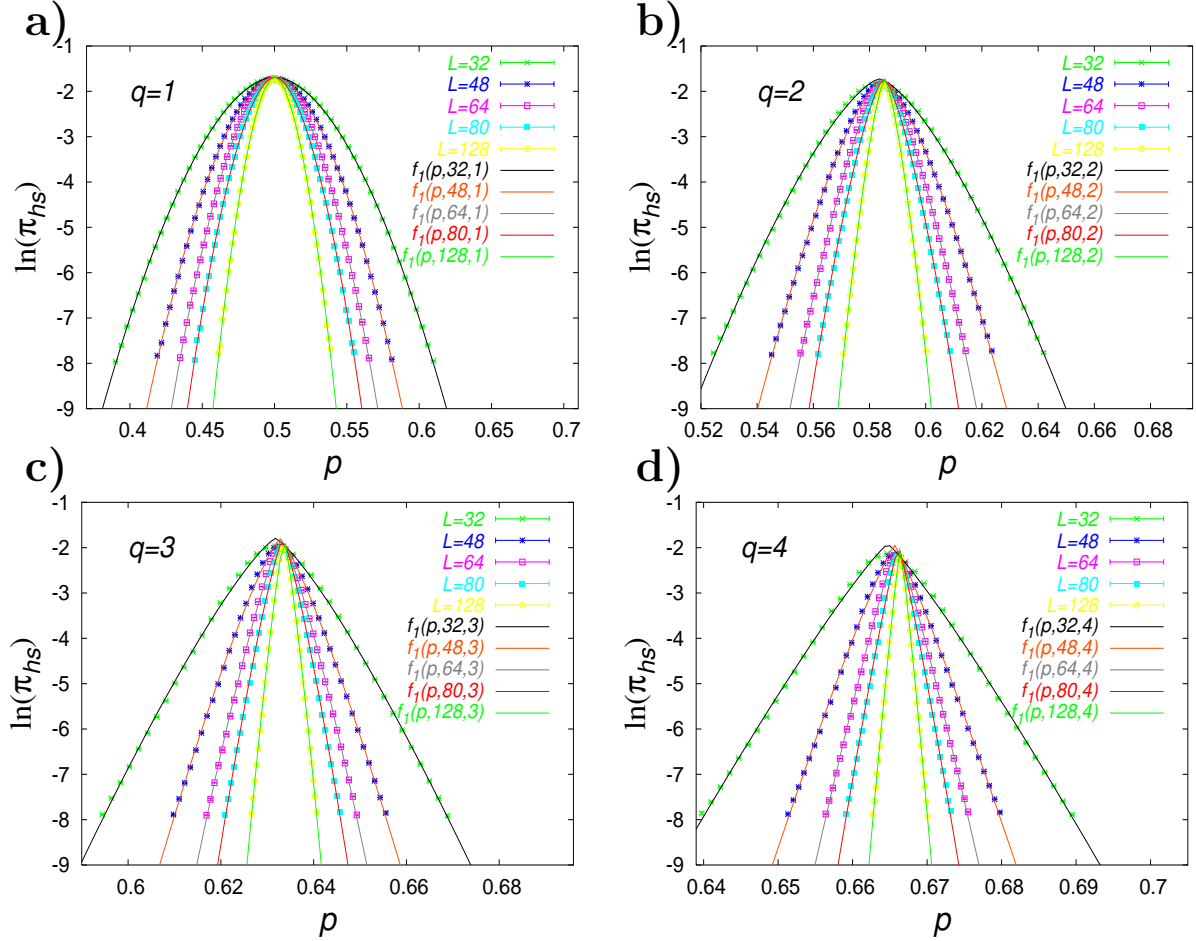


FIG. 3: Approximation of the logarithm of the crossing probabilities  $\ln(\pi_{hs})$  as a function of  $p$  by the function  $f_1(p; L, q) = \ln(A(q; L)) - b(q; L)(p - p_c(q; L))^{-\zeta(q; L)}$  for: a) percolation  $q = 1$ , b) Ising model  $q = 2$ , c) Potts model  $q = 3$ , d) Potts model  $q = 4$

by the function  $\tilde{b}(L, q)L^{u(L, q)}$ . In Fig.4a) the results of approximation are plotted by lines. In Table II the data for the scaling variable  $B(L, q)$  is shown. Values of the fitting parameters  $\tilde{b}(L, q)$ ,  $u(L, q)$  as well as the inverse correlation length index  $\frac{1}{\nu}$  are placed in the three last rows of Table II. We can see for  $q = 1, 2, 3$  that  $u(L, q) \simeq \frac{1}{\nu(q)}$ . It can be assumed that

$$B(L, q) = \tilde{b}(L, q)L^{\frac{1}{\nu(q)}} \quad (4)$$

In the case  $q = 4$  the scaling index  $u(q)$  is not equal  $\frac{1}{\nu(q=4)}$ . Many critical quantities in the Potts model  $q = 4$  exhibit logarithmic corrections [31, 32, 33, 34]. These logarithmic corrections explain the difference between analytical value  $\frac{1}{\nu(q=4)} = 1.5$  and numerical approximation for the scaling index  $y = 1.383(3)$ . The the position of the critical point as a function of the lattice size  $L$  is shown in Fig.4b). On the dual lattice the position of the critical point

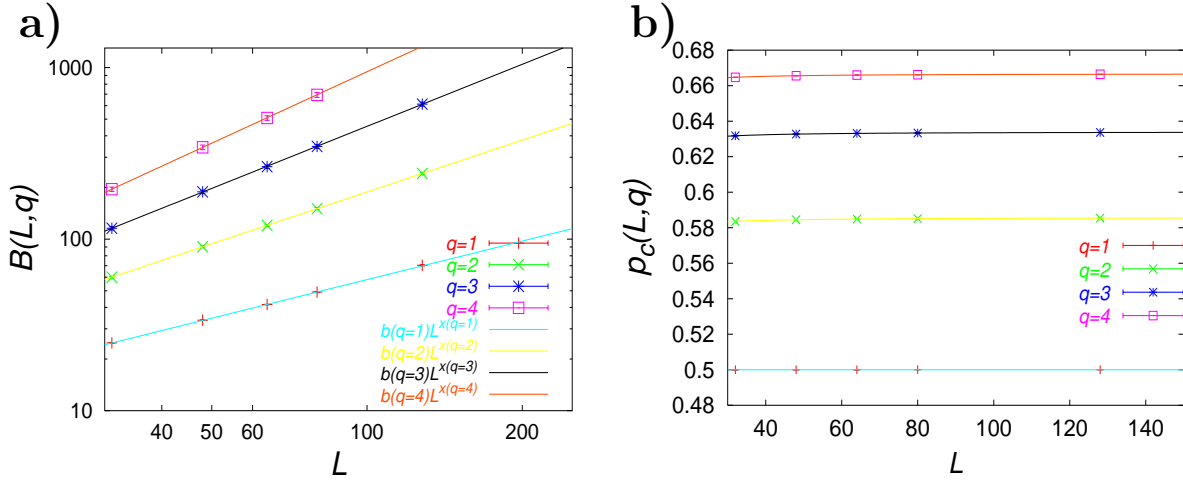


FIG. 4: a) The fitting parameter  $B(L, q)$  as a function of  $L$ . Results of the approximation by functions  $\tilde{b}(L, q)L^{u(L, q)}$  (see Table II) are plotted by lines. b) Position of the pseudocritical point on the finite lattice  $p_c(L, q)$  as a function of the lattice size  $L$  for  $q = 1, 2, 3, 4$  and approximation by the pow law  $p_c(L, q) = p_c(\infty; q) + dp(q)L^{v(q)}$  for  $q = 2, 3, 4$ . Line 0.5 is added also.

TABLE II: Data for  $B(L, q)$  and fitting parameters  $\tilde{b}(L, q)$ ,  $u(L, q)$

$L$	$q = 1$	$q = 2$	$q = 3$	$q = 4$
32	24.8(1)	60(1)	116(3)	195(6)
48	33.7(2)	90(1)	188(4)	343(11)
64	41.6(2)	120(2)	264(6)	508(16)
80	49.1(3)	150(2)	347(9)	693(23)
128	70.3(6)	241(4)	612(17)	1332(42)
$\tilde{b}(L, q)$	1.87(3)	1.849(6)	1.80(2)	1.62(2)
$u(L, q)$	0.746(3)	1.004(1)	1.201(3)	1.383(3)
$\frac{1}{\nu(q)}$	0.75	1	1.2	1.5

for percolation is equal  $\frac{1}{2}$  and does not depend on the lattice size. For our computation for all points  $p_c(L, q)$  the deviations from 0.5 are less than 0.0001. This deviation corresponds to numerical inaccuracy of our Monte-Carlo simulation. The data  $p_c(L, q)$  for  $q = 2, 3, 4$  were approximated by the power function of the lattice size  $p_c(L, q) \simeq p_c(q) + dp(q)L^{v(q)}$ . The results of approximation are placed in Table III and are also plotted by lines in Fig.4b). We shall see that our fitting procedure determine the critical point with accuracy up to four

TABLE III: Results of the approximation of  $p_c(L, q)$  by the power law  $p_c(q) + dp(q)L^{v(q)}$ . The analytical values  $p_c^{precise}(q) = \frac{\sqrt{q}}{\sqrt{q+1}}$  are added for comparison.

$q$	$dp(q)$	$v(q)$	$p_c(q)$	$p_c^{precise}(q)$
2	-0.25(2)	-1.37(3)	0.58572(2)	0.585786...
3	-0.30(2)	-1.43(2)	0.63392(1)	0.633975..
4	0.33(2)	-1.49(1)	0.66665(1)	0.6666666..

digits after the decimal point. So we shall use obtained values  $p_c(L, q)$  for following approximation of tails of the crossing probability. In Table IV we place results of the approximation for the index  $\zeta(L, q)$  describing the curvature of the central part of the crossing probability.

TABLE IV: Results of the approximation for  $\zeta(L, q)$

$L$	$q = 1$	$q = 2$	$q = 3$	$q = 4$
$\nu$	$4/3 \simeq 1.3333$	1	$5/6 \simeq 0.83333$	$2/3 \simeq 0.6666$
32	1.835(7)	1.436(13)	1.248(18)	1.139(19)
48	1.823(8)	1.432(13)	1.244(18)	1.133(20)
64	1.828(7)	1.432(14)	1.249(19)	1.134(20)
80	1.830(11)	1.430(15)	1.245(21)	1.131(21)
128	1.811(16)	1.429(16)	1.239(21)	1.130(20)

#### IV. THE SHAPE OF THE THE CROSSING PROBABILITY $\pi_{HS}$ TAILS: DIRECT APPROACH.

Let us check the shape of the crossing probability tails. The double logarithm of the crossing probability  $\ln(-\ln(\pi_{hs}(L, q)))$  are plotted as a functions of the variable  $t = \ln(|p - p_c(L, q)|)$  in Fig.5a), Fig.5b), Fig.5c), Fig.5d) for  $q = 1, 2, 3, 4$  respectively. Points for high-temperature and low-temperature tails lay on the same lines. This yields that we shall prove one more time our fitting procedure.

In the interval  $\ln(6) \leq \ln(-\ln(\pi_{hs}(L, q))) \leq \ln(12)$  the tails of the crossing probability looks like straight lines. Therefore we claim that the crossing probability tails are described

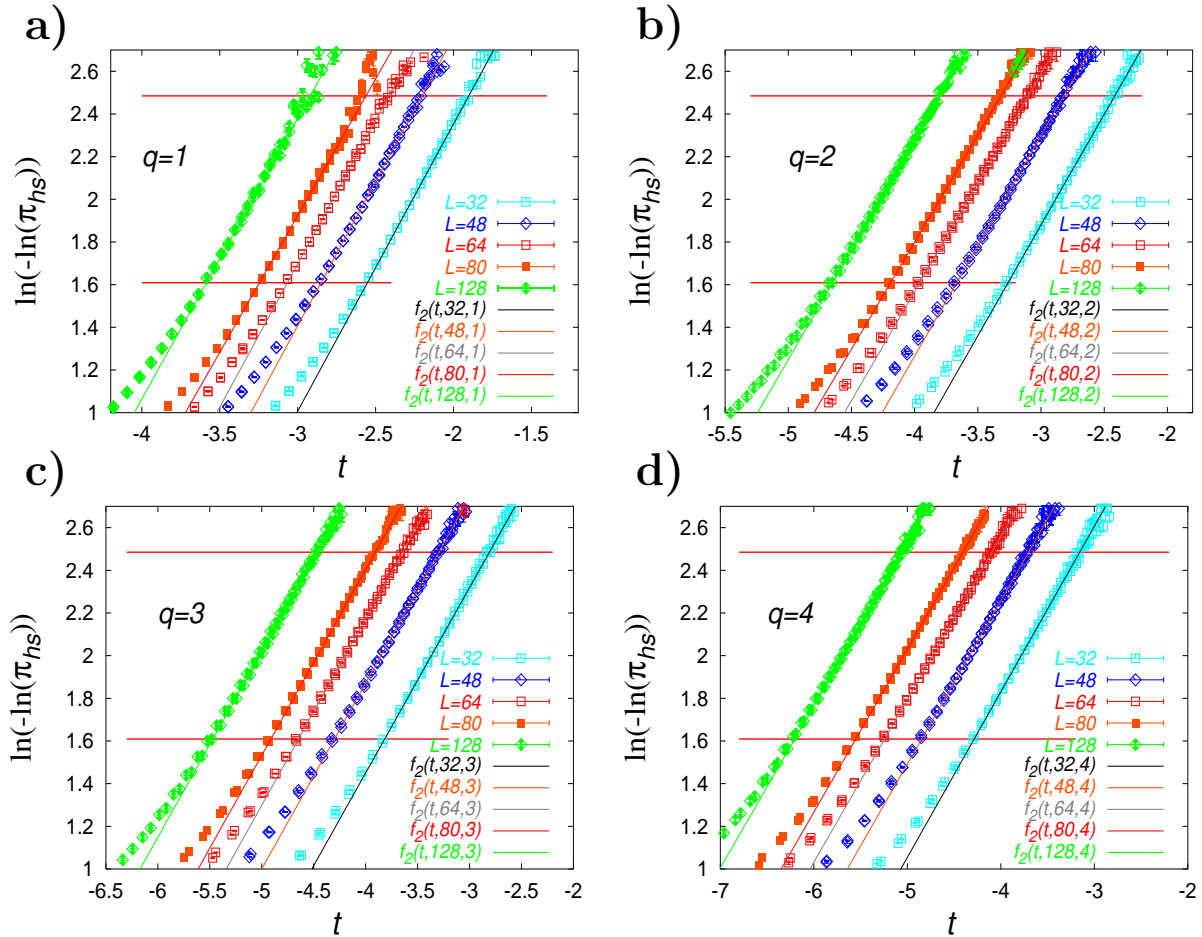


FIG. 5: Approximation of the double logarithm of the crossing probabilities  $\ln(-\ln(\pi_{hs}(p; L, q)))$  by the function  $f_2(t; L, q) = c(L, q) - d(L, q)t$  of the logarithm of the distance to the critical point  $t = \ln(|p - p_c(L, q)|)$ . for: a) percolation  $q = 1$ , b) Ising model  $q = 2$ , c) Potts model  $q = 3$ , d) Potts model  $q = 4$ . The range of the approximation is shown by the red horizontal lines.

by the formula

$$\pi_{hs}(p; L, q) = \exp\left(-C(L, q)(p - p_c(L, q))^{x(L, q)}\right) \quad (5)$$

We obtain the set of  $p_c(L, q)$  for  $L = 32, \dots, 128$  and  $q = 2, 3, 4$  in Section III. Using this data let us to approximate the double logarithm of tails  $\ln(-\ln(\pi_{hs}))$  as a function of  $t$  by formula (6).

$$f_2(t; L, q) = \tilde{c}(L, q) + x(L, q)t \quad (6)$$

Combining (5) and (6), we obtain  $\tilde{c}(L, q) = \ln(C(L, q))$ . The resolution of our computations  $10^{-7}$  is about 16 in  $(-\ln)$  scale and is about 2.7 in  $(\ln(-\ln))$  scale. We use the points in the interval  $\ln(6) < \ln(-\ln(\pi_{hs})) < \ln(12)$ ,  $\ln(6) \simeq 1.79$ ,  $\ln(12) \simeq 2.48$  for this approximation.

This interval is indicated in Fig.5a)-Fig.5d) by red horizontal lines. In this figures the slope lines represent results of approximation for  $x(L, q)$ .

In the region  $\ln(-\ln(\pi_{hs})) < \ln(6)$  the crossing probability obeys an another scaling low. In the region  $\ln(-\ln(\pi_{hs})) > \ln(12)$  the numerical inaccuracy becomes large. There are only a few numbers of "hits" in horizontally spanning clusters for  $\ln(-\ln(\pi_{hs})) > \ln(12)$ . Results of the numerical approximation for  $x(L, q)$  and  $\tilde{c}(L, q)$  are presented in Table V and Table VI respectively. As we can see that  $x(L, q) \simeq \nu(q)$ . Exception is the case  $q = 4$ . For  $q = 4$

TABLE V: The slope of lines: results of the approximation for  $x(L, q)$ , the analytical values  $\nu(q)$  are presented for comparison.

$L$	$q = 1$	$q = 2$	$q = 3$	$q = 4$
$\nu$	$4/3 \simeq 1.3333$	1	$5/6 \simeq 0.83333$	$2/3 \simeq 0.6666$
32	1.346(8)	1.038(6)	0.869(5)	0.776(6)
48	1.354(8)	1.034(8)	0.871(6)	0.766(4)
64	1.343(6)	1.021(11)	0.874(9)	0.763(4)
80	1.281(17)	1.004(14)	0.870(10)	0.764(4)
128	1.314(21)	1.026(17)	0.869(12)	0.760(5)

we obtain  $x(L, q = 4) \simeq 3/4$  instead of  $\nu(q = 4) = 2/3$ . This deviations may be explained by the logarithmic corrections. Some deviations exceeding the approximation errors can be explained by the choice of the approximation region. As it can be easily seen from Fig.5a)–Fig.5d) that decreasing of the bottom approximation bound  $\ln(6)$  cause decreasing of the slop of the approximation line. From all said above we can conclude that the tails of the crossing probability behaves like  $\exp(-(p - p_c)^\nu)$ . In Fig.6 the fitting parameter  $\tilde{c}(L, q)$  is plotted as a function of  $L$  for  $q = 1, 2, 3, 4$ . The line  $\ln(L) + 1.5$  is added for comparison. We fit the parameter  $\tilde{c}(L, q)$  by the expression  $\tilde{c}_1 + \tilde{c}_2 \ln(L)$  and show results in Table VII. We may assume that the parameter  $\tilde{c}_2$  for  $q = 2, 3, 4$  is equal 1 within accuracy of the approximation. Therefore we may assume that

$$\pi_{hs}(p; L, q) \simeq \exp\left(-c(q)L[p - p_c(L, q)]^{\nu(q)}\right) \quad (7)$$

In Fig.1a) we show the crossover from the behavior in the vicinity of the critical point to the tails. Namely, we plot the data  $-\ln(\pi_{hs})$  for  $q = 2, L = 128$  as a function of the variable

TABLE VI: Shift of the lines: results of the approximation  $\tilde{c}(L, q)$ 

$L$	$q = 1$	$q = 2$	$q = 3$	$q = 4$
32	5.063(18)	4.974(21)	4.961(20)	4.919(19)
48	5.476(18)	5.374(14)	5.357(13)	5.325(15)
64	5.762(25)	5.666(14)	5.645(15)	5.590(12)
80	5.885(45)	5.890(14)	5.884(15)	5.815(11)
128	6.331(76)	6.364(15)	6.350(18)	6.299(16)

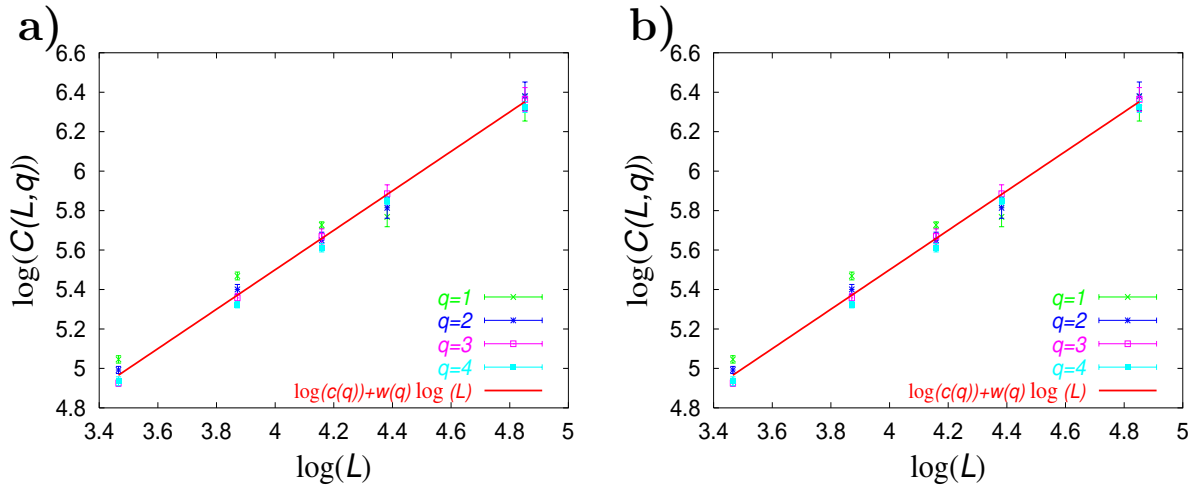


FIG. 6: a) The fitting parameter  $\tilde{c}(L, q)$  (the vertical shift of the approximation lines) as a function of  $L$  (ln scale on the axis  $L$ ) for  $q = 1, 2, 3, 4$ . The function  $\ln(L) + 1.5$  is added for comparison. b) Position of the pseudocritical point on the finite lattice  $p_c(L, q)$  as a function of the lattice size  $L$  for  $q = 1, 2, 3, 4$  and approximation by the power law  $p_c(L, q) = p_c(\infty; q) + dp(q)L^{v(q)}$  for  $q = 2, 3, 4$ . Line 0.5 is added also.

$\tau = L(p - p_c(L, q))^\nu$ . We shall call the function under consideration in the vicinity of the critical point a "body" of the crossing probability on the contrary the "tails" of the crossing probability. In Fig.1) we plot also results of the approximation of the crossing probability by functions (3) and (6). The fitting parameters are taken from Table I, Table II, Table IV, Table V and Table VI.

TABLE VII: Results of the approximation of  $\tilde{c}(L, q)$  by the function  $\tilde{c}_1 + \tilde{c}_2 \ln(L)$ 

$q$	1	2	3	4
$\tilde{c}_1$	1.8(2)	1.66(12)	1.29(4)	1.43(5)
$\tilde{c}_2$	0.93(6)	0.96(3)	1.05(1)	1.007(11)

## V. NEW FITTING PROCEDURE

From all said above we can make the following conclusions. There are two scaling regions: the one is in the vicinity of the critical point, and the second is the tails. Analyzing formula (2), (4) and (7) we can conclude that the distance from the critical point  $(p - p_c(L, q))$  and the lattice size  $L$  occurs in a formula only as combination  $L/\xi \sim L(p - p_c(L, q))^{\nu(q)}$  in accordance with scaling theory. Let us introduce a scaling variable

$$\tau = L(p - p_c(L, q))^{\nu(q)} \quad (8)$$

If we plot the negative logarithm of the crossing probability  $-\ln(\pi_{hs})$  as a function of the scaling variable  $\tau$  than we expect the power dependence in the vicinity of zero and linear dependence for tails, as we can see in Fig.1. We can use the scaling variable  $\tau = L(p - p_c(L, q))^{\nu(q)}$  to fit the crossing probability taking into account the finite size scaling. Let us describe a new fitting procedure.

We may assume that we obtain the position of the critical point on the finite lattice  $p_c(L, q)$  and the logarithm of the amplitude  $a(L, q)$  as a result of the previous fit. We take the fitting parameter  $a(L, q)$  and the critical point position  $p_c(L, q)$  from Table I and Table III. So we can use only two free fitting parameters and fix the value  $p_c^*(L, q)$  and  $a^*(L, q)$ . The asterisk denote that we fix variables  $p_c^*(L, q)$  and  $a^*(L, q)$  and do not varyate them during the fitting procedure. Substituting (8) for  $\tau$  in (3) and (5), we obtain fitting formula for the body and the tails of the crossing probability

$$-\ln(\pi_{hs}) \simeq f_3(\tau; L, q) = -a^*(L, q) + b(L, q)\tau^{z(L, q)} \quad (9)$$

$$-\ln(\pi_{hs}) \simeq f_4(\tau; L, q) = c(L, q)\tau^{y(L, q)} \quad (10)$$

If our assumptions are right then the fitting parameters don't depend on the lattice size  $L$  and the parameter  $y$  must be equal to 1.

The numerical value of the variable  $p_c(L, q)$  is used for computation of  $t$  in accordance with (8). Comparing the new fitting procedures (9), (10) and the previous fitting procedures (3), (5) we can obtain relations between the new fitting parameters  $b(L, q)$ ,  $z(L, q)$ ,  $c(L, q)$  and parameters  $\tilde{b}(L, q)$ ,  $\zeta(L, q)$ ,  $C(L, q)$

$$b(q) = \tilde{b}(q)^{\zeta(q)}(q) \quad (11)$$

$$z(q) = \frac{\zeta(q)}{\nu(q)} \quad (12)$$

$$C(L, q) = \ln(c(L, q)) + \ln(L), \quad \tilde{c}_1(L, q) = \ln(c(L, q)) \quad (13)$$

The special case is  $q = 4$ . As we can see from the results of the approximations in Table II and Table V the finite size scaling of the crossing probability for  $q = 4$  does not obey the scaling law  $L(p - p_c)^{\nu(q=4)}$  (probably to logarithmic corrections to scaling). Therefore instead of the analytical value  $\nu(q = 4) = 2/3$  we use the numerical approximation  $x(q = 4) = 3/4$  from Table V. We can see later, that this substitution let us to obtain correct results for scaling.

We perform the fitting procedure in accordance with the formula proposed above. For the fit of the body of the crossing probability (9) the scaling region  $1.6 < -\ln(\pi_{hs}) < 6$  was used. For the fit of the tails of the crossing probability (10) we use the scaling region  $6 < -\ln(\pi_{hs}) < 12$ . We place results of the fitting procedure for  $q = 1, 2, 3, 4$  in Fig.7a), Fig.7b), Fig.7c), Fig.7d) respectively. In this figures the fitting regions are denoted by horizontal lines. As we expect, if we plot the data as functions of the scaling variable  $\tau$  then the finite size dependence eliminates and points for different values of  $L$  lies on the same curve. Results of the approximation for the fitting parameters  $b(L, q)$ ,  $z(L, q)$ ,  $c(L, q)$  and  $y(L, q)$  are collected in Table VIII, Table IX, Table X, Table XI respectively.

The data for  $b(L, q)$  in Table VIII demonstrates, that this fitting parameter does not depend on the lattice size  $L$ . All dependence on  $L$  is enclosed in the expression for  $\tau$ . Hence we can omit the variable  $L$  in the round brackets and consider  $b(q)$  only as a function of  $q$ . This fact proved the choice of the fitting procedure. The data in Table IX presents some power  $z(q)$ . This power describes the behavior of the crossing probability in the vicinity of the critical point as a function of the scaling variable  $\tau$  and does not depend on the lattice size. The dependence of the crossing probability as a function of the distance to the critical point  $p - p_c$  is described by the index  $\zeta(q) = z(q)\nu(q)$ . The data for the fitting parameter

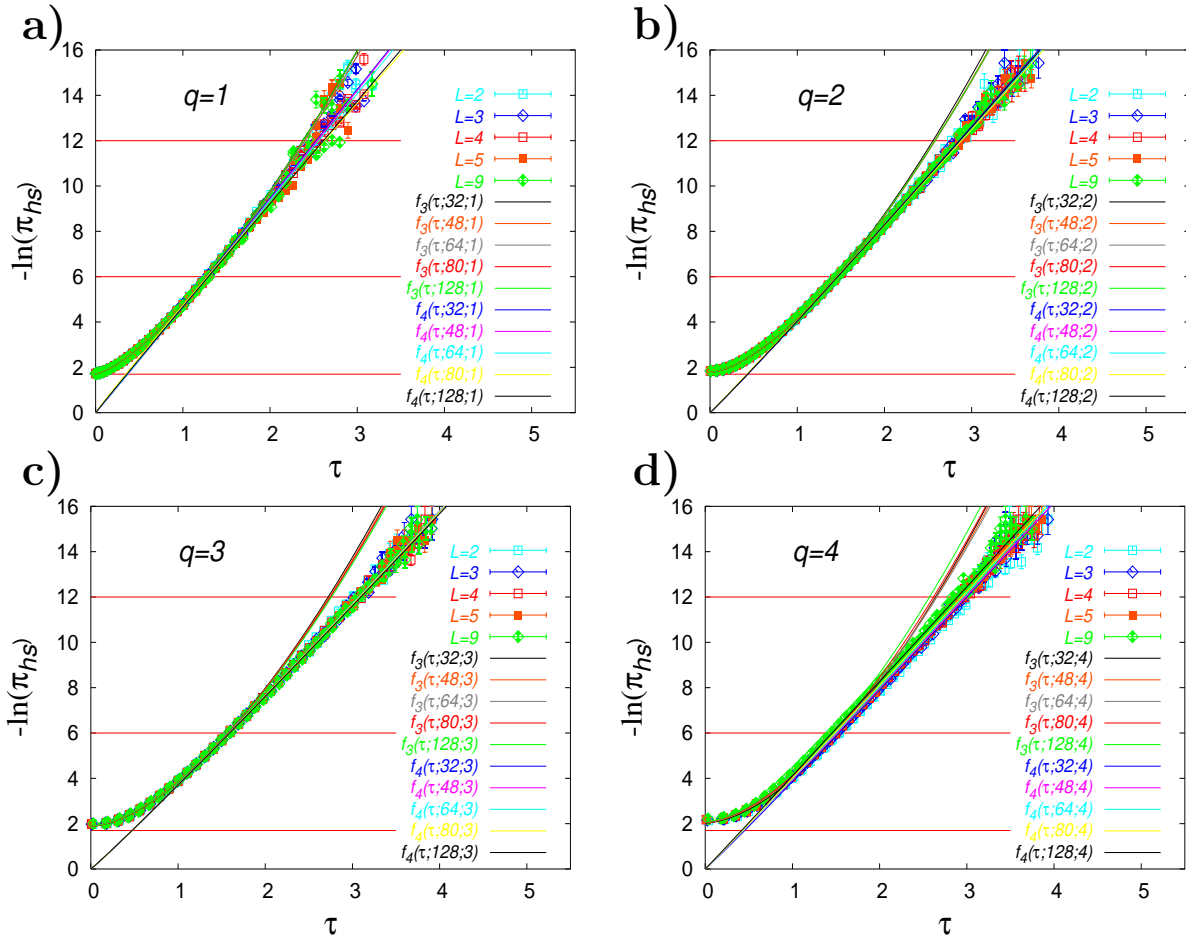


FIG. 7: The logarithm of the crossing probability  $-\ln(\pi_{hs}(p; L, q))$  as a function of the the scaling variable  $\tau = L(p - p_c(L, q))^{\nu(q)}$ . for: a) percolation  $q = 1$ , b) Ising model  $q = 2$ , c) Potts model  $q = 3$ , d) Potts model  $q = 4$ . Results of the approximation of the body of the crossing probability by the function  $f_3(\tau; L, q) = a(L, q) + b(L, q)\tau^z$  and the tails of the crossing probability by the function  $f_4(\tau; L, q) = c(L, q)\tau^y$ . The ranges of approximations are shown by the horizontal lines.

$c(L, q)$  are placed in Table X. It seems, that this parameter does not depend on  $L$ . The results for  $y(L, q)$  is placed in Table XI. We can see that  $y$  equal 1. This fact demonstrate the exponential dependence of the crossing probability tails as a function of the scaling variable. The data in Table XI confirm assumption of the stretched exponential behavior of the tails of the crossing probability.

TABLE VIII: Results of the approximation for the fitting parameter  $b(L, q)$ 

$L$	$q = 1$	$q = 2$	$q = 3$	$q = 4$
32	3.044(4)	2.356(11)	1.882(13)	1.856(15)
48	3.033(4)	2.356(12)	1.865(14)	1.917(14)
64	3.018(3)	2.345(12)	1.881(15)	1.937(16)
80	3.024(6)	2.345(11)	1.885(14)	2.009(13)
128	3.029(7)	2.349(14)	1.873(16)	2.023(19)

TABLE IX: Results of the approximation for the fitting parameter  $z(L, q)$ 

$L$	$q = 1$	$q = 2$	$q = 3$	$q = 4$
32	1.411(4)	1.577(10)	1.697(16)	1.760(21)
48	1.396(5)	1.570(11)	1.709(19)	1.707(17)
64	1.402(4)	1.576(10)	1.681(19)	1.691(18)
80	1.430(3)	1.566(10)	1.677(17)	1.665(17)
128	1.423(4)	1.580(13)	1.668(19)	1.693(23)

## VI. DISCUSSION

The using the dual lattice (see Fig.2) let us to avoid finite size shift of the critical point for the bond percolation and to diminish it for the spin models. The accuracy of definition of the critical point on the finite lattice play the principal role for the investigation of the tails scaling. The high quality of our approximation is proved by remarkable symmetry of the crossing probability with respect to the critical point  $p_c$ . In Fig.5 the points for two branches  $p - p_c > 0$  and  $p - p_c < 0$  practically coincides.

The two different scaling region of the crossing probability clearly seen in fig.1a) can explain the long time uncertainty about its shape. In Ref.[21] the scaling index for the percolation threshold for  $2d$  percolation model was found  $\zeta \simeq 1.9(1)$ . This result is in formal coincidence with our approximation of the body of the crossing probability for percolation  $\zeta \simeq 1.82(2)$ . In more recent works [10, 16, 17, 18, 19] the tails region was investigated which is described by the scaling law  $\exp(-cL(p - p_c)^{\nu=4/3})$ . The crossover form to Gaussian-like behavior to slope  $4/3$  is observed in figures of Ref.[22].

TABLE X: Results of the approximation for the fitting parameter  $c(L, q)$ 

$L$	$q = 1$	$q = 2$	$q = 3$	$q = 4$
32	4.70(1)	4.04(1)	3.72(1)	3.85(2)
48	4.66(1)	4.05(2)	3.70(2)	3.93(1)
64	4.66(1)	4.08(3)	3.70(3)	3.97(1)
80	4.74(3)	4.12(3)	3.70(3)	4.00(1)
128	4.66(4)	4.06(4)	3.68(4)	4.09(2)

TABLE XI: Results of the approximation for the fitting parameter  $y(L, q)$ 

$L$	$q = 1$	$q = 2$	$q = 3$	$q = 4$
32	1.009(6)	1.037(6)	1.042(6)	1.034(8)
48	1.015(6)	1.034(8)	1.046(7)	1.022(5)
64	1.007(4)	1.021(11)	1.049(11)	1.018(6)
80	0.960(13)	1.004(14)	1.045(12)	1.019(5)
128	0.984(15)	1.027(17)	1.043(14)	1.013(6)

We have five fitting parameters  $a(q, L), b(q), z(q), c(q)$ . in expressions (9) and (10). In Fig.7a)-Fig.7d) we see the crossover region between the body and the tails of the crossing probabilities. In this region the function  $f_3$  touched the line  $f_4$ . It means, that in some point  $\tau_0$  this functions are equal

$$-a(L, q) + b(q)\tau_0^{z(q)} = c(q)\tau_0 \quad (14)$$

and first derivatives of this functions are equal too.

$$z(q)b(q)\tau_0^{z(q)-1} = c(q) \quad (15)$$

From (15) we can express the value of  $\tau_0$

$$\tau_0 = \left( \frac{c(q)}{b(q)z(q)} \right)^{\frac{1}{z(q)-1}} \quad (16)$$

Substituting (16) in (14) we obtain formula

$$a(L, q) = b(q) \left( \frac{c(q)}{b(q)z(q)} \right)^{\frac{z(q)}{z(q)-1}} - c(q) \left( \frac{c(q)}{b(q)z(q)} \right)^{\frac{1}{z(q)-1}} \quad (17)$$

If the crossing probabilities at the critical points  $A(q)$  (and logarithms  $a(q)$ ) can be calculated analytically by conformal field methods [2, 3, 4] than only two independent parameters  $b(q)$  and  $z(q)$  are remains for the crossing probability. The main statements for the crossing probability  $\pi_{hs}$  are:

- In accordance with scaling theory the finite size scaling of the crossing probabilities may be eliminated by introducing the scaling variable  $\tau = L(p - p_c(L, q))^{\nu(q)}$ . The crossing probability as functions of  $\tau$  does not depend on the lattice size  $L$ .
- The body of the crossing probability scales  $\pi_{hs}(\tau) \simeq A(L, q) \exp(-b(q)\tau^{z(q)})$ .
- The tails of the crossing probabilities scales  $\pi_{hs}(\tau) \simeq \exp(-c(q)\tau)$
- The finite size scaling for  $q = 4$  does not describe by the analytical value of the correlation length index  $\nu(q = 4) = 2/3$ . We obtain some scaling index  $x(q = 4)$ . This index  $x(q = 4) \simeq 0.75$  for the tails of the crossing probability (Table V) or  $\frac{1}{u(q)} \simeq 0.723$  for the body of the crossing probability (Table II).

The author would like to thank Robert M. Ziff for helpful discussion.

- 
- [1] C.M. Fortuin and P.M. Kasteleyn, *Physica* **57**, 536 (1972).
- [2] J.L. Cardy, *Nucl. Phys. B* **275**, 200 (1986).
- [3] J.L. Cardy, *J. Phys. A* **25**, L201 (1992).
- [4] G.M.T. Watts, *J.Phys. A* **29**, L363 (1996).
- [5] S. Smirnov, W. Werner, e-print: math.PR/0109120.
- [6] S. Smirnov, *C. R. Acad. Sci. Paris Sr. I Math.* **333**, 239 (2001).
- [7] J.L. Cardy, e-print: cond-mat/0209638.
- [8] R.P. Langlands, C. Pichet, P. Pouliot, and Y. Saint-Aubin, *J. Stat. Phys.* **67**, 533 (1992).
- [9] R.P. Langlands, Ph. Pouliot, Y. Saint-Aubin, *Bull. AMS* **30**, 1 (1994).
- [10] R. M. Ziff, *Phys. Rev. Lett.*, **72**, 1942 (1994).
- [11] Ch.-K. Hu, C.-Yu Lin, J.-A.Chen , *Phys. Rev. Lett.* **75**, 193 (1995).
- [12] Ch.-K. Hu, Chai-Yu Lin, *Phys. Rev. Lett.* **77**, 8 (1996).
- [13] C.-Yu Lin, Ch.-K. Hu, *Phys. Rev. E*, **58**, 1521 (1998).

- [14] C.-K. Hu, J.-A. Chen C.-Y. Lin, *Physica A*, **266**, 27 (1999).
- [15] R. P. Langlands, M.-A. Lewis, Y. Saint-Aubin, *J.Stat.Phys.* **98**, 131 (2000).
- [16] M. E. J. Newman and R. M. Ziff, *Phys. Rev. Lett.*, **85**, 4104 (2000).
- [17] M. E. J. Newman and R. M. Ziff, *Phys. Rev. E*, **64**, 016706 (2001).
- [18] J. Berlyand and J. Wehr, *Journal of Physics A*, **28**, 7127 (1995).
- [19] J.-P. Hovi and A. Aharony, *Phys. Rev. E*, **53**, 235 (1996).
- [20] Levinshtein, B.I. Shklovskii, M.S. Shur and A.L. Efros, *Sov. Phys. JETP*, **42**, 197 (1976).
- [21] F. Wester, *Int. J. Mod. Phys. C*, **11**, 843 (2000).
- [22] P.M.C. de Oliveira, R.A. Nobrega and D. Stauffer, e-print: cond-mat/0308566.
- [23] R. J. Baxter "*Exactly Solved Models in Statistical Mechanics.*", Academic Press, 1982
- [24] R.M. Ziff, M.E. Newmann, *Phys. Rev. E* **66**, 016129 (2002).
- [25] R.M. Ziff, cond-mat/9710104.
- [26] J. Hoshen and R. Kopelman, *Phys. Rev. B* **14**, (1976) 3438.
- [27] U. Wolff, *Phys. Rev. Lett.*, Vol. **62**, 361 (1988).
- [28] D.P. Landau, *Phys. Rev. B* **13**, 2997 (1976).
- [29] D.P. Landau, *Phys. Rev. B* **14**, 255 (1976).
- [30] O.A. Vasilyev, *Phys. Rev. E*, 68, 026125 (2003).
- [31] J.L. Cardy, M. Nauenberg, D.J. Scalapino, *Phys. Rev. B* **22** 2560 (1980)
- [32] J. Salas, A.D. Sokal *J. Stat. Phys* **92** 729 (1998)
- [33] J. Asikainen, A. Aharony, B. B. Mandelbrot, E. M. Rauch, J.-P. Hovi *Eur. Phys. J. B* **34**, 479 (2003), e-print: cond-mat/0212216.
- [34] J. Cardy, R. Ziff, cond-mat/0205404